Realtime fermions in an anisotropic plasma

Maximilian Attems

Frankfurt Institute of Advanced Studies
1207.5795, 1301.7749, 1302.5098, 1401.XXX

Collaborators: Anton Rebhan, Michael Strickland;
Owe Philipsen, Christian Schäefer

New Frontiers in QCD 2013, November 2013

HELMHOLTZ ASSOCIATION

HIC for FAIR
Helmholtz International Center

Filamentation instability

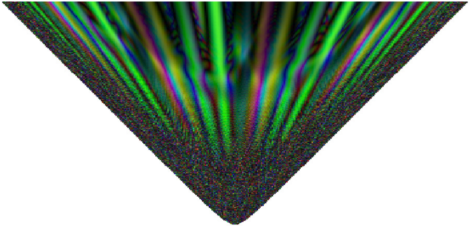

[MA, Rebhan, Strickland 2008]

Motivation

Filamentation instability

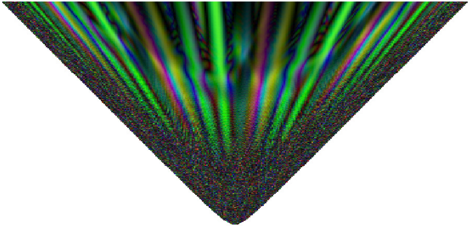

[MA, Rebhan, Strickland 2008]

- Hard Thermal Loop (HTL)
  $\alpha_s \approx 0.3$

Motivation

Filamentation instability

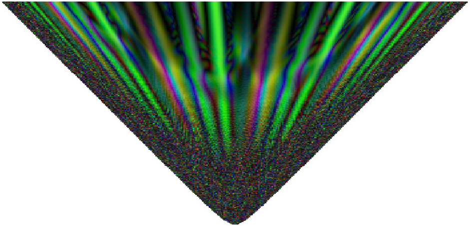

[MA, Rebhan, Strickland 2008]

- Hard ~~Thermal~~ Loop (H~~T~~L)
  $\alpha_s \approx 0.3$
- Real-time physical quantities of non-equilibrium processes

Motivation

Filamentation instability

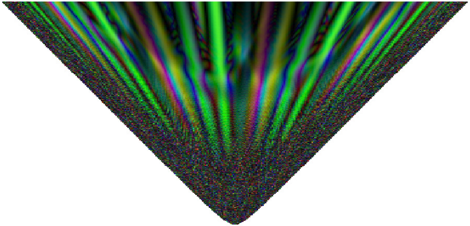

[MA, Rebhan, Strickland 2008]

- Hard ~~Thermal~~ Loop (H~~T~~L)
  $\alpha_s \approx 0.3$
- Real-time physical quantities of non-equilibrium processes
- Plasma turbulence affects parton transport (isotropization, jet energy loss, viscosity,..)
- Derivation of time scales for isotropization, thermalization

Outline

1. Hard Expanding Loops (HEL)
   - Stages of a heavy ion collision
   - High occupancy
   - Scales of wQGP
   - Weibel instabilities
   - Yang-Mills Vlasov
   - Bjorken expansion
   - Unstable modes growth rate
   - Unstable Color Glass Condensate

2. Physical Observables
   - Numerical tests
   - Energy densities
   - Pressures
   - Spectra
   - Longitudinal temperature

Stages of an heavy ion collision

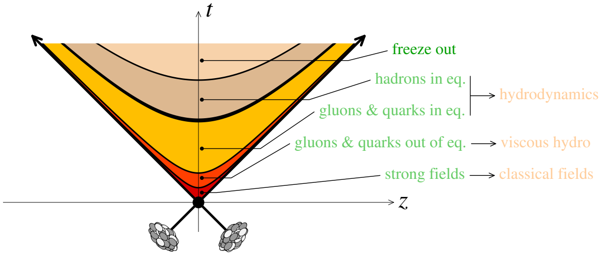

[Gelis 2006] Illustration of the stages of a heavy ion collision.

Stages of an heavy ion collision

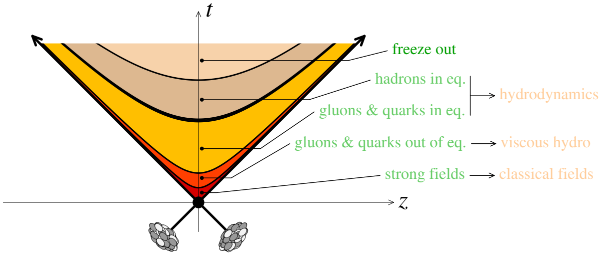

[Gelis 2006] Illustration of the stages of a heavy ion collision.

Numerical approaches to early phase with strong fields:

1. Numerical solution of Yang Mills equations in real-time: [Romatschke, Venugopalan; Berges, Sexty; Gelis, Fukushima; Dusling; Dumitru, Nara, Schenke; Moore, Kurkela; Epelbaum; Schlichting]
2. Hard Loop Simulation (Eikonalized particles): [Strickland, Romatschke, Rebhan; Arnold, Lenaghan, Moore; Mrowczynski; Rummukainen, Bödeker; Ipp, Attems; Deja]

High occupancy

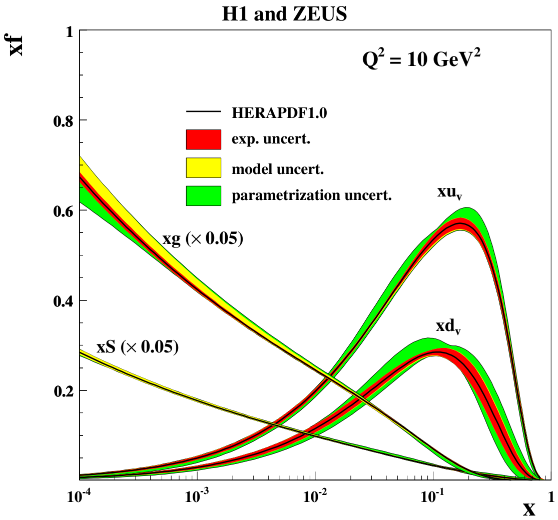

[H1, ZEUS Collaborations 2010] parton distribution functions

Scales of wQGP

Equilibrium:

- T: energy of hard particles
- gT: thermal masses, Debye screening mass,
- $g^2 T$: magnetic confinement, color relaxation, rate for small angle scattering
- $g^4 T$: rate for large angle scattering, $\eta^{-1} T^4$

Scales of wQGP

Non-Equilibrium:

- p_{hard}: energy of hard particles

- gA_μ: thermal masses, Debye screening mass,
  plasma instabilities [Mrowczynski 1988, 1993, ..]

Weibel instabilities

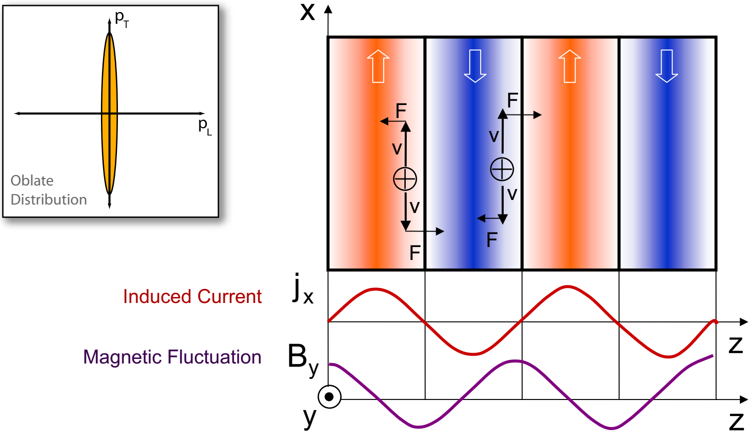

[Mrowczynski 1993; Strickland 2006]: Illustration of the mechanism of filamentation instabilities with Lorentz force.

Yang-Mills Vlasov

[Heinz 1985; Blaizot, Iancu 1993] One solves the covariant Vlasov

$$V \cdot D\, \delta f^a \Big|_{p^\mu} = g V^\mu F^a_{\mu\nu} \partial^\nu_{(p)} f_0(\mathbf{p}_\perp, p_\eta)$$

[Heinz 1985; Blaizot, Iancu 1993] One solves the covariant Vlasov

$$V \cdot D\, \delta f^a \Big|_{p^\mu} = g V^\mu F^a_{\mu\nu} \partial^\nu_{(p)} f_0(\mathbf{p}_\perp, p_\eta)$$

coupled to Yang-Mills

$$D_\mu F_a^{\mu\nu} = j_a^\nu = g\, t_R \int \frac{d^3p}{(2\pi)^3} \frac{p^\mu}{2p^0} \delta f_a(\mathbf{p}, \mathbf{x}, t)$$

with the Ansatz $\delta f(x; p) = -g W_\beta(x; \phi, y) \partial^\beta_{(p)} f_0(p_\perp, p_\eta)$

Yang-Mills Vlasov

[Heinz 1985; Blaizot, Iancu 1993] One solves the covariant Vlasov

$$V \cdot D\, \delta f^a \Big|_{p^\mu} = g V^\mu F^a_{\mu\nu} \partial^\nu_{(p)} f_0(\mathbf{p}_\perp, p_\eta)$$

coupled to Yang-Mills

$$D_\mu F^{\mu\nu}_a = j^\nu_a = g\, t_R \int \frac{d^3p}{(2\pi)^3} \frac{p^\mu}{2p^0} \delta f_a(\mathbf{p}, \mathbf{x}, t)$$

with the Ansatz $\delta f(x; p) = -g W_\beta(x; \phi, y) \partial^\beta_{(p)} f_0(p_\perp, p_\eta)$ using the longitudinal free streaming background distribution function

$$f_0(\mathbf{p}, x) = f_{\mathrm{iso}}\left(\sqrt{p_\perp^2 + (\frac{p'^z \tau}{\tau_{\mathrm{iso}}})^2}\right)$$

resulting in the plasma anisotropy

$$\xi = \frac{1}{2} \frac{\langle p_T^2 \rangle}{\langle p_z^2 \rangle} - 1\,, \quad \xi = (\tau / \tau_{\mathrm{iso}})^2 - 1.$$

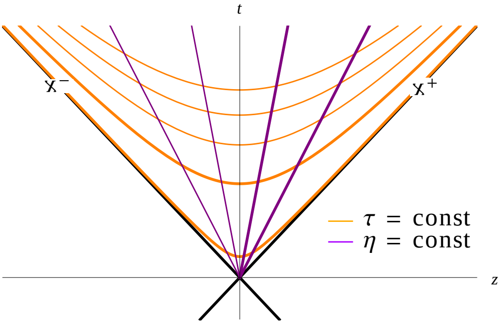

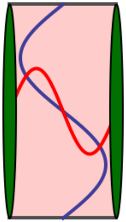

It is convenient to switch to comoving coordinates

$$t = \tau \cosh \eta\,, \qquad \tau = \sqrt{t^2 - z^2}\,,$$

$$z = \tau \sinh \eta\,, \qquad \eta = \mathrm{arctanh}\frac{z}{t}\,,$$

with the corresponding metric

$$ds^2 = d\tau^2 - d\mathbf{x}_\perp^2 - \tau^2 d\eta^2\,.$$

Unstable modes growth rate

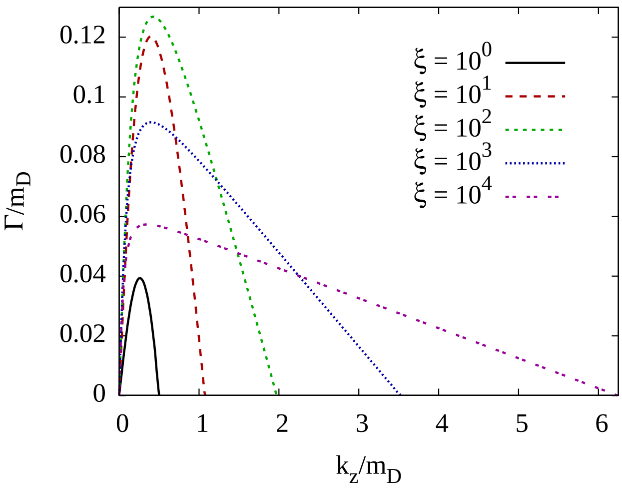

[Romatschke, Strickland 2003] Unstable mode spectra of purely longitudinal modes: $N(\tau) \approx \exp(2m_D\sqrt{\tau\tau_{\mathrm{ISO}}})$.

Unstable Color Glass Condensate

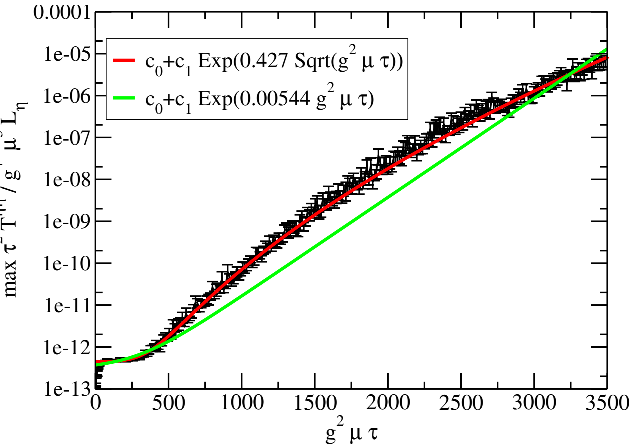

[Romatschke, Venugopalan 2006] NLO Color Glass Condensate (CGC) longitudinal pressure sees chromo-Weibel exp growth.

Unstable Color Glass Condensate

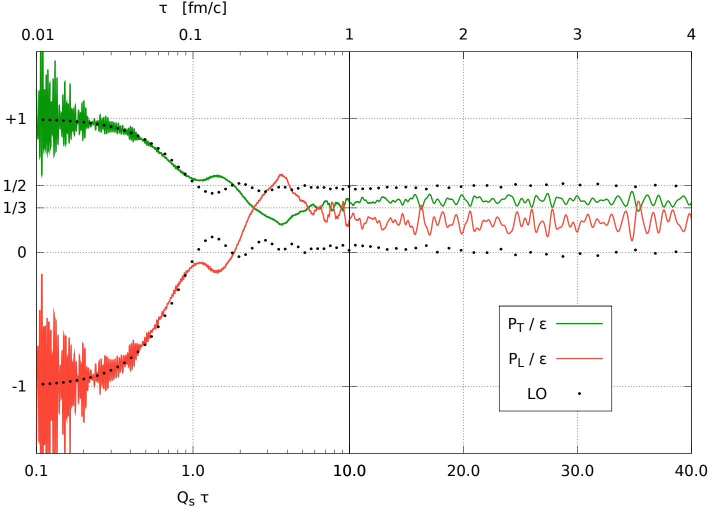

[Epelbaum, Gelis 2013] CGC NLO spectrum pressure evolution
[McLerran, Venugopalan (1993)] $T^{\mu\nu}_{CGC,LO} = diag(\mathcal{E}, \mathcal{E}, \mathcal{E}, -\mathcal{E})$.

Numerical setup

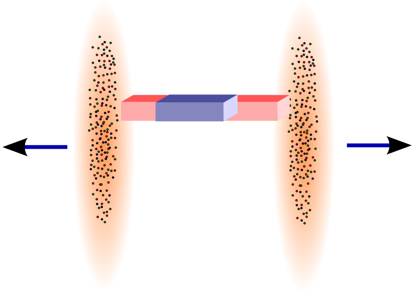

SU(2) particle content

$Q_s = 2\mathrm{GeV}$
Extrapolate to $\alpha_s \sim 0.3$

Initial gluon densities given by the gluon liberation factor $c = 2\ln 2$ [Kovchegov 2001].

lattice size for leapfrog EOM:

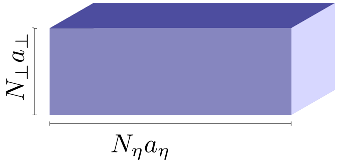

$N_\eta \times {N_\perp}^2 \times N_u \times N_\phi =$
$128 \times 40^2 \times 128 \times 32$
$a_\eta = 0.025,\ a_\perp Q_s = 1$
$\tau_0 = 1/Q_s$
$a_\tau = 10^{-2}\tau_0$

$$n(\tau_0) = c\frac{N_g Q_s^3}{4\pi^2 N_c \alpha_s(Q_s\tau_0)}$$

Computational challenge

Real-time lattice simulations distributed on the cluster:

Vienna Scientific Cluster:

Loewe Scientific Computing:

The code scales to 1-4k CPU's using OpenMPI for $> 10^{10}$ auxiliary fields organised in 5-dimensional matrices on sites.

Outline

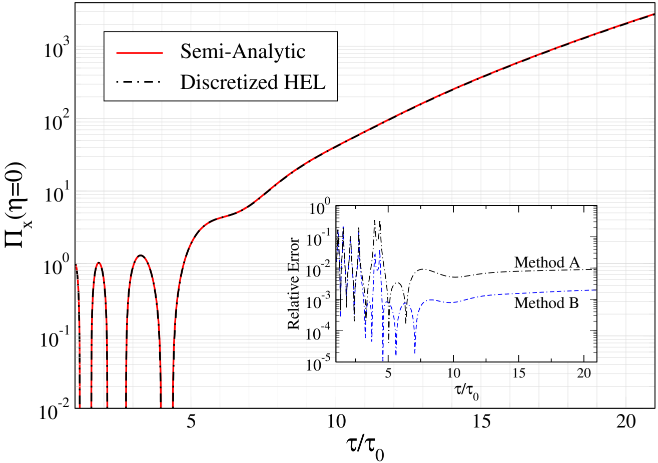

[MA, Rebhan, Strickland 2008] Abelian single mode evolution the conjugate momentum comparison with [Romatschke, Rebhan 2006]

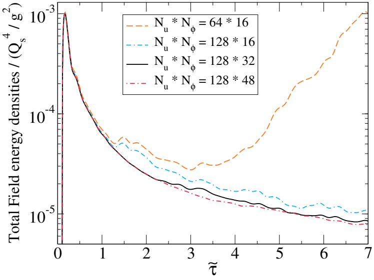

Evolution of stable modes

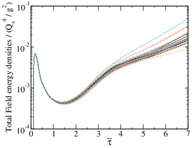

(a) Different seeds

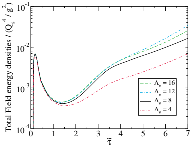

(b) Variation of Λ_ν

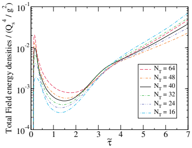

(c) Variation of $a_\perp$

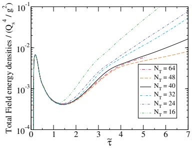

(d) Variation of $N_\perp$

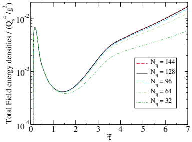

(e) Variation of a_η

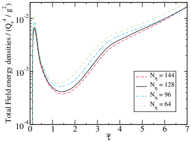

(f) Variation of N_η

Energy densities fields

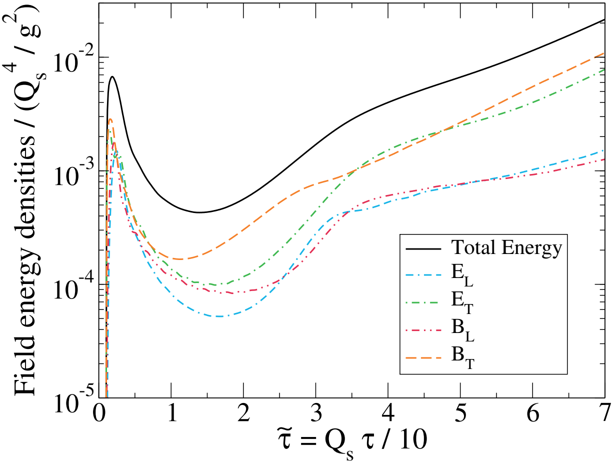

50 averaged runs $N_\perp * N_\eta * N_u * N_\phi = 40^2 * 128 * 128 * 32$:
after onset one sees **rapid growth** of $\mathbf{B}_T$ and $\mathbf{E}_T$ **fields**, followed by non-Abelian interactions kicking in.

Energy densities fields

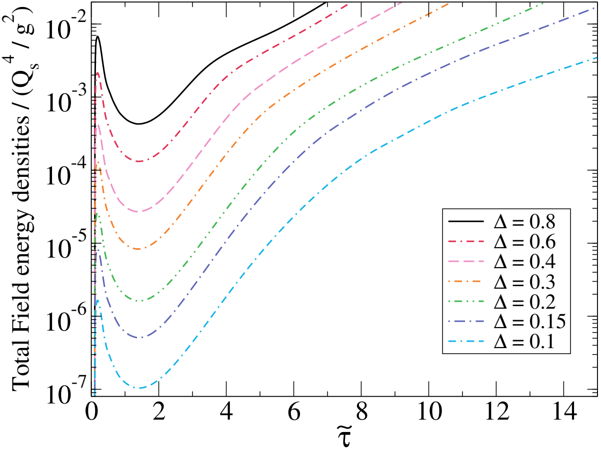

Total field energy density for different initial current fluctuation magnitudes.

Pressures

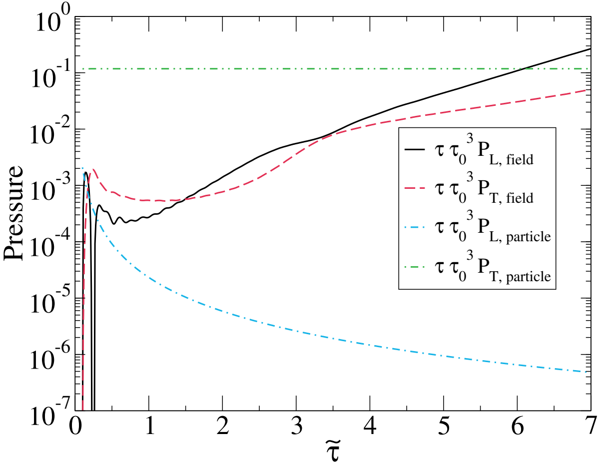

Initially highly anisotropic, note $P_{L,\text{field}}(\tau = 0.3) < 0$, **growing field pressures**, $P_{L,\text{field}}$ dominates at late times, $\tilde{\tau}$ scaled P_L drops $\propto 1/\tilde{\tau}^2$.

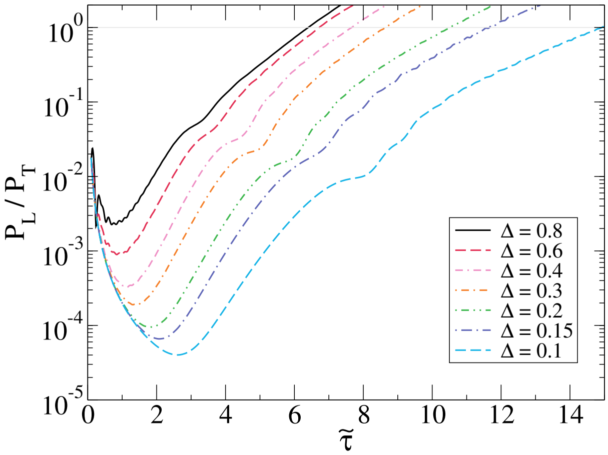

The evolution of the total longitudinal pressure over the total transverse pressure for different initial current fluctuation magnitudes Δ.

Spectra

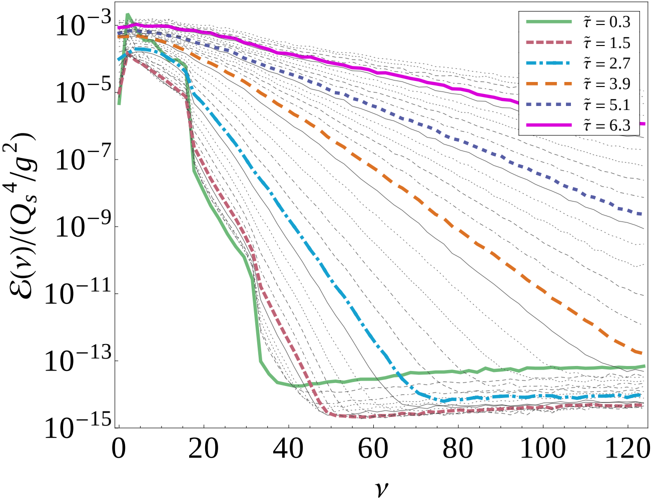

The longitudinal energy spectra at various proper times over the longitudinal wavenumber $\nu = k_z * \tau$: **rapid emergence of an exponential distribution of longitudinal energy**.

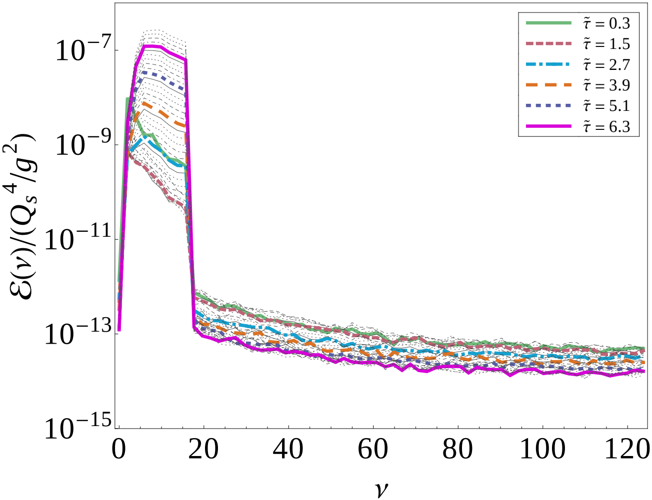

Longitudinal spectra for **abelian** runs shows amplification of the initial seeded modes.

Spectra

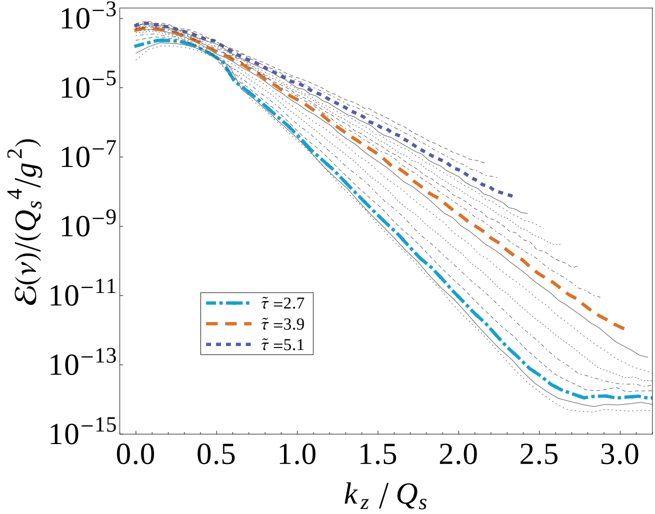

The **red-shifting** is even more visible in the k_z plot. Nonlinear mode-mode coupling is vital in order to populate high momentum modes.

Massless Boltzmann distribution fits the longitudinal spectra:

$$\mathcal{E}_{\mathrm{fit}}(k_z) = A\left(k_z^2 + 2|k_z|T + 2T^2\right)\exp\left(-|k_z|/T\right) \qquad (1)$$

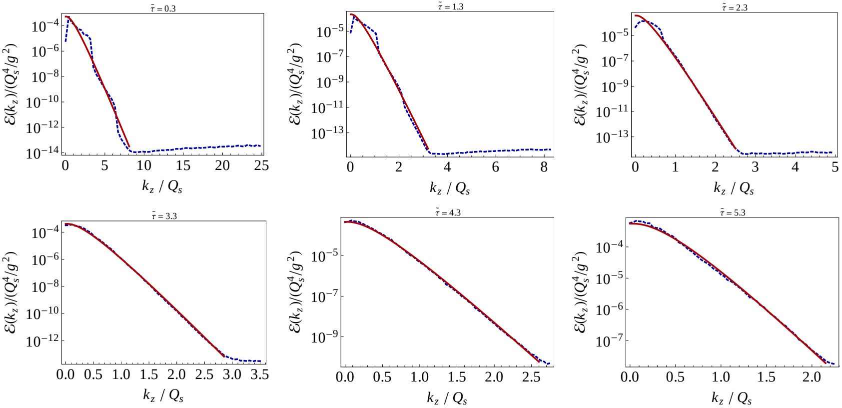

Comparison of data and fit function at six different $\tilde{\tau}$.

Longitudinal thermalization

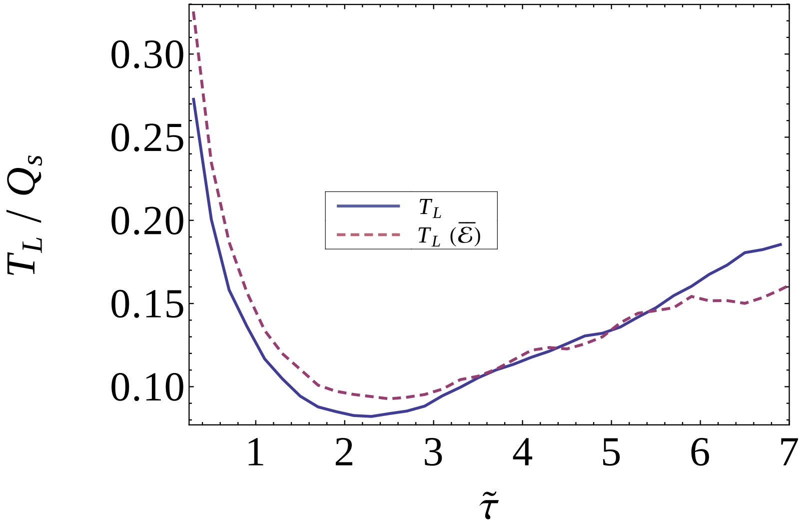

After initial cool down **instabilities reheat** longitudinal soft fields.

Filamentation instability

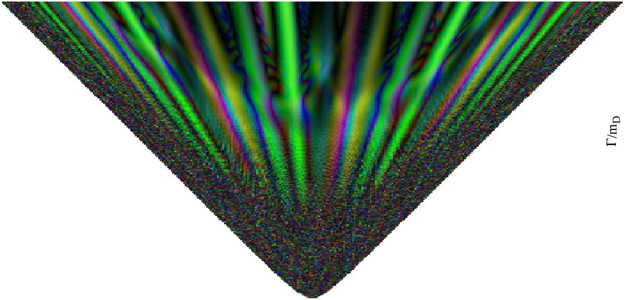

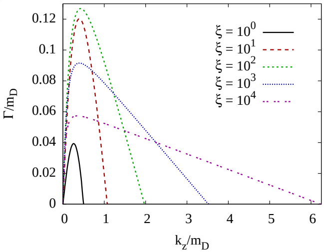

[2008 Rebhan, Strickland, A.] Visualization of the 1D+3V space-time development of color correlations in a non-Abelian plasma instabilities in Bjorken expansion.

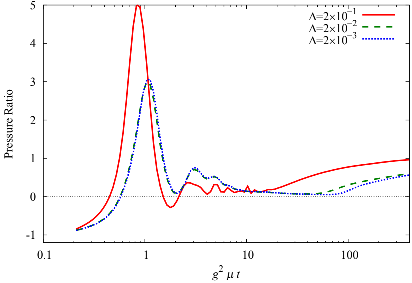

SU(2) [Fukushima 2013]

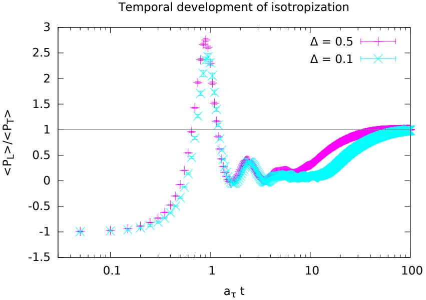

SU(3) [MA, Philipsen, Schäfer 2014]

Isotropization at later time is a very slow process even in a non-expanding and symmetric box.

CGC IC Yang-Mills Box

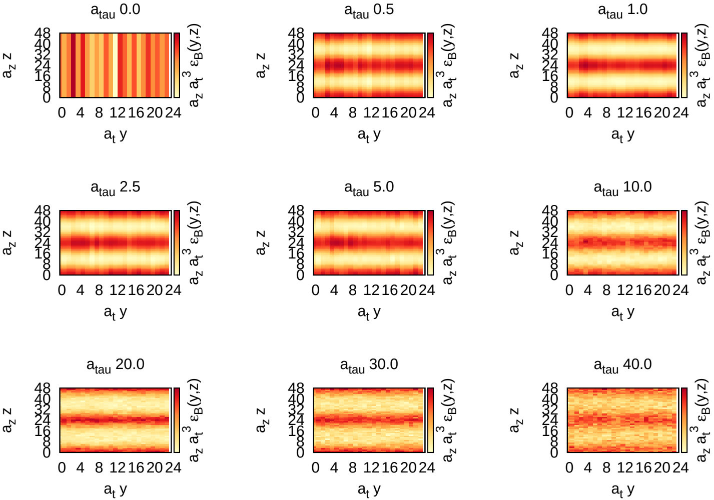

Local energy density of B_x at different times.

Stochastic Fermions

- Quantum mechanical treatment via mode function expansion [Aarts, Smit 1998]
- Introduce two kinds of fermions: Male and female

$$D(x,y) = \left\langle \psi_M(x)\bar{\psi}_F(y) \right\rangle = \left\langle \psi_F(x)\bar{\psi}_M(y) \right\rangle \,.$$

$$(i\gamma^\mu\partial_\mu - m + g\Re\Phi(x) - ig\Im\Phi(x)\gamma^5)\psi_g(x) = 0\,.$$

- Define Fourier transformed stochastic fields

$$\psi_g(\vec{p}) = \int_{\vec{x}} e^{ip_jx^j}\psi_g(\vec{x}), \quad \psi_g(\vec{x}) = \int_{\vec{p}} e^{-ip_jx^j}\bar{\psi}_g(\vec{p})\,. \qquad (2)$$

- Simulate ladder operators with complex random numbers ξ and η [Borsanyi, Hindmarsh 2009]

Conclusions

- We performed the **first real-time 3d numerical** study of non-Abelian plasma in a longitudinally expanding system within the discretized hard loop framework:
  hard expanding loops HEL.
- Extrapolating our results to energies probed in ultrarelativistic heavy-ion collisions we find, however, that a **pressure anisotropy** persists for a few fm/c.
- The longitudinal spectra seem to be well described by a Boltzmann distribution indicating **rapid longitudinal thermalization of the gauge fields** $\tau_{\mathrm{thermal}} \sim 1 \quad \mathrm{fm/c}$.
- There doesn't seem to be a "soft scale" saturation of the instability as was seen in static boxes.
- Simulations with $N_\eta = 2048$ confirm our numerical results. We are also studying Yang-Mills dynamics with fermions.

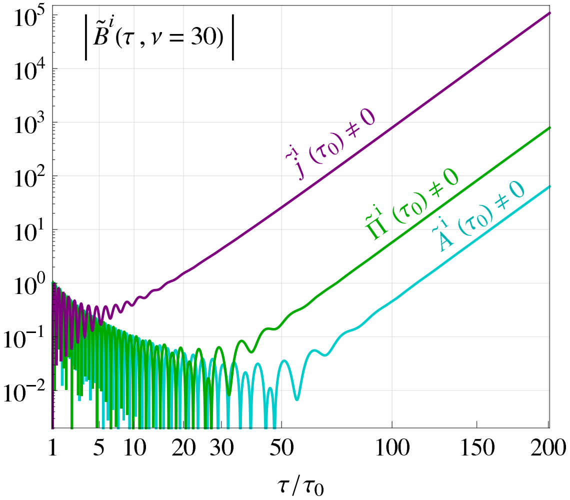

[Rebhan, Steineder 2009] IC variation for specific mode $\nu = 30$